

## Structure of $O_2^-$

M. J. W. Boness and G. J. Schulz

*Mason Laboratory, Yale University, New Haven, Connecticut 06529*

(Received 25 May 1970)

Measurements of the differential cross section for the elastic scattering of low-energy electrons by  $O_2$  at  $50^\circ$  exhibit structure resulting from the compound state  $O_2^-$ . From these observations we calculate the spectroscopic constants of the ground state  ${}^2\Pi_g$  of  $O_2^-$ , and we find the values  $\omega_e(O_2^-) = 1089 \text{ cm}^{-1}$  and  $r_e(O_2^-) = 1.377 \text{ \AA}$ . A portion of the potential-energy curve of the  $O_2^-({}^2\Pi_g)$  is plotted using the Morse-function representation and our calculated values of the spectroscopic constants.

### I. INTRODUCTION

This paper presents measurements of the differential cross section for the elastic scattering of low-energy electrons by molecular oxygen. The structure observed in these data is interpreted in terms of a temporary negative-ion state. Since we measure the elastic cross section alone, without any interference from vibrational excitation taking place in the same energy range, the present experiment removes any possible ambiguity regarding the nature of the observed structure. We combine the spacing of the structure in the elastic cross section with various other complementary data to determine the spectroscopic constants  $\omega_e$  (vibrational frequency for infinitesimal amplitudes) and  $r_e$  (equilibrium internuclear separation) for  $O_2^-$  and to calculate the lower portion of the potential-energy curve for  $O_2^-$ . The data are consistent with the existence of a single bound state of  $O_2^-$ , presumably in the  $X^2\Pi_g$  configuration.

### II. EXPERIMENT

The apparatus used for the present study consists of two  $127^\circ$  electrostatic selectors which serve as an electron monochromator and an analyzer, respectively. The apparatus is similar to a previously described instrument,<sup>1</sup> an important difference being the ability to rotate the monochromator, thus offering the capability of angular distribution studies. The monochromator produces an electron beam of approximately  $10^{-8} \text{ \AA}$  at 1.5 eV with a full width at half-height of approximately 60 meV. This beam is accelerated or retarded to the desired impact energy and then crossed with a molecular beam within the collision chamber where single-collision conditions prevail. For the present experiment, the second electrostatic analyzer is positioned at a fixed scattering angle of  $50^\circ$  and operated in such a way that it transmits those electrons which are elastically scattered into its acceptance angle. Following the energy analysis, the electrons are detected by a helical Bendix channeltron multiplier. This signal

is amplified by an electrometer and displayed as a function of electron impact energy on an X-Y plotter.

### III. RESULTS

Figure 1 shows the experimental results; namely, the energy dependence of the elastically scattered current at approximately  $50^\circ$ . The energy scale is established by flowing a mixture of  $O_2$  and He and observing the location of the  $He^-(1s2s^2)$  resonance whose position is accurately known to be<sup>1</sup> 19.30 eV. The energy scale thus established is believed to be accurate within  $\pm 0.1$  eV. The differential elastic cross section shown in Fig. 1 exhibits structure consisting of five peaks whose spacings (starting from low energy and measured to the nearest 10 meV) are 0.12, 0.12, 0.11, and 0.11 eV. These observations are consistent with a previous transmission experiment performed by Boness and Hasted<sup>2</sup> and with the more recent work of Hasted and Awan.<sup>3</sup> More recently, this structure has been confirmed by Spence and Schulz<sup>4</sup> operating a trapped-electron tube in such a way as to observe the total scattering cross section. For purposes of comparison, all four measurements are shown together in Fig. 1, though it should be pointed out that each curve represents a different type of measurement. We had to shift the energy scale of the transmission experiments to obtain agreement with the present data. We attribute the structure shown in Fig. 1 to resonance-scattering resulting from a temporary negative-ion state whose vibrational spacings are represented by the separation of adjacent peaks.

The fact that the structure in the elastic cross section appears to originate from 0 eV, coupled with the fact that a stable negative ion  $O_2^-$  is known to exist, indicates that the structure we observe represents the higher-lying vibrational levels of this negative-ion state. This identification is further endorsed when we qualitatively compare the difference between the values of the spectroscopic constant  $\omega_e$  of the negative-ion and neutral system with the predicted variation based upon their different molecular orbital configurations. According to Mulliken<sup>5</sup>

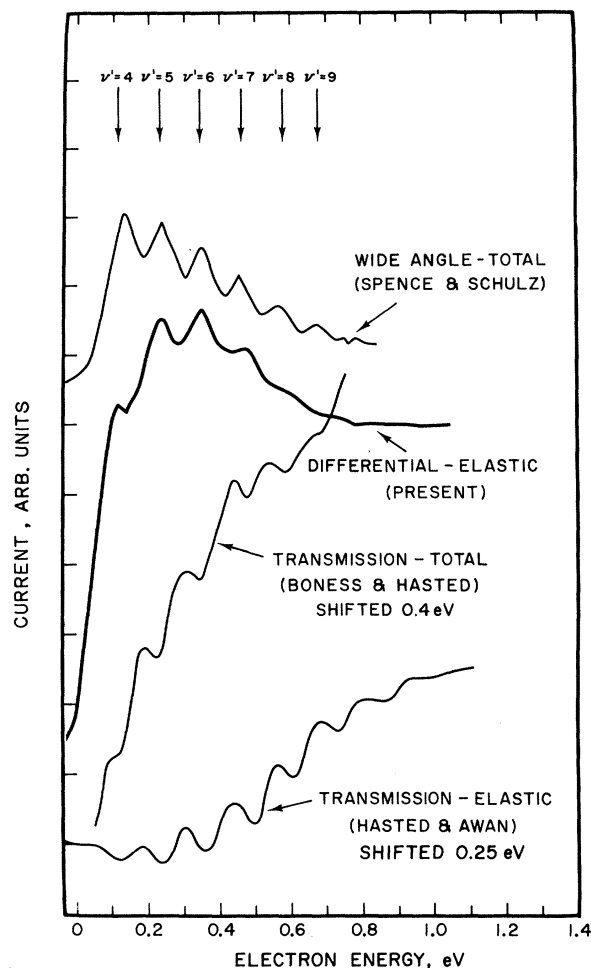


FIG. 1. Comparison of four experiments on the structure in the low-energy cross section of  $O_2^-$ . The type of experiment and the authors are indicated for the four curves. The top two curves represent the wide-angle total and the small-angle differential cross section, respectively. The bottom two curves represent transmission experiments. The latter two experimental curves had to be shifted by 0.4 and 0.25 eV, respectively, in order to overlap the present results. This does not appear unreasonable in view of the poor control of the energy scale in these experiments. It should be noted that a rise in the differential cross section represents a dip in the transmission and the transmission curves were shifted until a good match could be obtained. The agreement between the structure shown on the four curves is considered to be good. The indicated quantum numbers refer to the  $O_2^-$  system.

and Bates and Massey,<sup>6</sup> the ground-state configuration of  $O_2^-$  corresponds to the ground-state configuration of the neutral  $O_2$ , ( ${}^3\Sigma_g^-$ ), plus an additional electron accommodated in a  $\pi_g$  orbital. The antibonding nature of this orbital leads to a smaller force constant, and hence to a smaller value of  $\omega_e$  for the  $O_2^-$  system compared to the  $O_2$  configuration. This is consistent with the experimental observations. It

is important to consider the possibility of excited-state configurations such as those proposed by Bates and Massey,<sup>6</sup> whose configurations may be obtained by applying the Wigner-Witmer correlation rules<sup>7</sup> to the states of the separated atoms. According to Mulliken,<sup>5</sup> none of these states is likely to be in the energy range of interest, and indeed no experimental evidence exists for bound excited states derived from the lowest dissociation limit.<sup>8</sup>

#### IV. EVALUATION OF $\omega_e$

An approximate value for  $\omega_e(O_2^-)$  can be obtained from the separation between adjacent peaks of the differential cross section. However, these spacings include anharmonicity effects which should be eliminated if a precise value of  $\omega_e$  is required. The spacing between any two vibrational levels  $\nu'$  and  $\nu' - 1$  is given by  $\Delta E_{\nu', \nu'-1} = hc(\omega_e - \nu'2\omega_e x_e)$ . The anharmonicity  $\omega_e x_e$  can be taken as one-half the difference between the spacings of adjacent peaks of the elastic cross section (0.0015 eV). To arrive at the proper value for  $\omega_e$ , we need to know the particular quantum number associated with a given peak in the elastic cross section. To establish these quantum numbers, it is necessary to extrapolate the observed sequence of peaks back to  $\nu' = 0$ . The cutoff point for the sequence below 0 eV is determined by the value of the electron affinity of  $O_2$ .

We can begin the extrapolation from any of the peaks observed in the differential cross section; however, since the accuracy of our energy-scale calibration is comparable with the separation of adjacent peaks, it is possible to make an error of  $\pm 1$  in the quantum-number assignments. In order to avoid such an error, we have used the finding that the  $\nu = 3$  level of  $O_2$  is accidentally coincident<sup>4</sup> with one of the vibrational levels  $\nu'_x$  of  $O_2^-$ . This level is then used as the starting point for the extrapolation.

For the spacing of the first two vibrational levels of the sequence,  $\nu'_x$  and  $\nu'_x - 1$ , we have used the value<sup>4</sup> of 0.111 eV which offers higher accuracy than our measured value of 0.11 eV. For twice the anharmonicity  $2\omega_e x_e$ , the value 0.003 eV is used which is consistent both with our results and those of Spence and Schulz and close to the value suggested by Holzer *et al.*<sup>9</sup>

Finally, to perform the extrapolation, a value for the electron affinity of  $O_2$  is required. We find in the literature 16 determinations for the electron affinity of  $O_2$ . The theoretical values range from 0.15 to 1 eV. However, since theory lacks the accuracy and reliability for such a complicated calculation, one should look to experiments for a guide. Unfortunately, experiments show a similar range of values, and thus one must review critically the experiments with the hope that the experiment to

which we can find least objection yields the proper value for the electron affinity. The experiments can be divided into four categories; namely, determinations of appearance potentials by electron impact ( $O_2^-/O_3$  and  $O_2^-/NO_2$ ), charge-transfer reactions, photodetachment, and attachment-detachment reactions. The *appearance potential* measurements give values for the electron affinity in excess of<sup>10</sup> 0.58 eV ( $O_2^-/O_3$ ) and<sup>11</sup> 1.1 eV ( $O_2^-/NO_2$ ), respectively. However, it has recently been shown that appearance potentials for negative-ion formation in triatomic molecules can depend on gas temperature and can lead to spuriously high values of the electron affinity.<sup>12</sup> We therefore consider these experiments inconclusive at the present time.

The *thermal detachment reaction*<sup>13</sup>  $O_2^- + O_2(^1\Delta_g) \rightarrow 2O_2 + e$  leads to an upper limit of 0.97 eV and the absence of a *thermal charge-transfer reaction*<sup>14</sup>  $H^+ + O_2 \rightarrow H + O_2^-$  at 300°K leads to an upper limit of 0.78 eV. A study of *high-energy charge-transfer reactions*<sup>15</sup> in the energy range 3–80 eV ( $H^+ + O_2 \rightarrow O_2^- + H$ ;  $SO^+ + O_2 \rightarrow O_2^- + SO$ ;  $ND_2^+ + O_2 \rightarrow O_2^- + ND_2$ ) leads to a lower limit of 1.05 eV and an upper limit of 1.2 eV. The latter method relies upon the identification of the reaction kinetics (i. e., whether it is exothermic or endothermic) from the shape of the cross-section curve in the energy range 3–80 eV. However, the shape of the cross section in this energy range is probably not a reliable guide for identifying the reaction kinetics, and serious doubt must be expressed regarding validity of this approach.<sup>16</sup> The upper limit for the electron affinity of  $O_2$  from *photodetachment*<sup>17</sup> experiments is 0.53 eV and an extrapolation using Geltman's<sup>18</sup> threshold theory yields a value of 0.15 eV. Uncertainties in this determination arise from the possibility that vibrationally excited species of  $O_2^-$  contribute to the photodetachment signal and also from the long extrapolation needed to reach the threshold. The *drift-tube studies of attachment and detachment coefficients*<sup>19</sup> in thermal equilibrium are also possibly affected by the participation of vibrationally excited species. However, the large number of collisions (about  $10^6$ ) and the absence of any change in the value of the electron affinity as the oxygen density is changed, indicates that vibrationally excited species probably do not play a role in this determination. Thus, we accept for the present the value given by Pack and Phelps<sup>19</sup> (0.43 eV) for the electron affinity of  $O_2$ .

By using the values of the quantities discussed above to perform the extrapolation of the vibrational sequence to  $\nu' = 0$ , we find that the value for the quantum number of the  $O_2^-$  vibrational level which is coincident with the  $\nu = 3$  level of  $O_2$  is  $\nu'_x = 8$ . Thus we find a value for the spacing of the first two vibrational levels of  $O_2^-$ ,  $\nu' = 1 \rightarrow \nu' = 0$  of 0.132 eV. This value agrees closely with the value of 0.135

eV deduced from the measurement<sup>9</sup> of the Raman frequency for the free  $O_2^-$  species embedded in alkali-halide crystals. This spacing expressed in wave numbers is equal to  $\omega_e - 2\omega_e x_e$  and hence  $\omega_e$  ( $O_2^-$ ) is 1089  $cm^{-1}$  or 0.135 eV. Terminating the backward extrapolation of the vibrational spacings for  $O_2^-$  at the energy nearest the value of the electron affinity of Pack and Phelps, leads to a value of 0.40 eV, which overlaps within experimental error the value of Pack and Phelps.

## V. EVALUATION OF $r_e$

A number of empirical formulas<sup>7</sup> exist relating the equilibrium internuclear separation  $r_e$  to  $\omega_e$ . The most commonly accepted and most versatile of these is Badger's rule,<sup>20</sup> which is given by the relation  $r_e = (C_{ij}/k_e)^{1/3} + d_{ij}$ , where  $k_e = 4\pi^2\mu^2c^2\omega_e^2$  is the force constant,  $\mu$  is the reduced mass, and  $e$  is the velocity of light.  $C_{ij}$  and  $d_{ij}$  are empirical constants which are characteristic of all diatomic molecules which consist of one atom in the  $i$ th long row and one in the  $j$ th long row of the periodic system. For  $i = j = 1$  (i. e.,  $O_2^-$  among many others) the values of the empirical constants are  $C = 1.86 \times 10^5$  dyn  $cm^{-1}$  and  $d_{ij} = 0.680$  Å. Employing these values, Badger finds that in only one case out of the 35 considered does the error in determining  $r_e$  exceed 0.05 Å and for 21 of these cases the error is less than 0.025 Å.

Using the above values for the empirical constants and the value of  $\omega_e(O_2^-)$  determined previously, we find the value for the equilibrium internuclear separation  $r_e(O_2^-) = 1.377$  Å.

## VI. POTENTIAL-ENERGY CURVE FOR $O_2^-$

Finally, we wish to use these combined experimental and calculated data to present a potential-energy diagram. We use the Morse-function representation<sup>21</sup> for the potential-energy curves. Using this formulation, the potential energy is given by

$$U(r - r_e) = D_e(1 - e^{\beta(r_e - r)})^2$$

where  $r$  is the internuclear separation and  $r_e$  its equilibrium value,  $D_e$  the dissociation energy referred to the minimum (not  $\nu = 0$ ) of the curve, and  $\beta$  is given by the expression  $\beta = \omega_e(2\pi^2c\mu/D_e h)^{1/2}$ , where  $h$  is Planck's constant, and the other symbols are as previously defined.

Figure 2 shows the potential-energy curves calculated for  $O_2(X^3\Sigma_g^-)$  and for the  $O_2^-$  state. The spectroscopic constants for the  $O_2$  system are taken from Herzberg,<sup>7</sup> and the potential-energy curve for  $O_2$  agrees extremely well with the curve calculated by Gilmore<sup>22</sup> using a numerical modification of the Rydberg-Klein method. The dissociation energy of  $O_2^-$  is deduced from our knowledge of the electron affinity of  $O_2$ , the electron affinity of O and the dissociation energy for  $O_2$  which yields  $D_e(O_2^-) = 4.083$

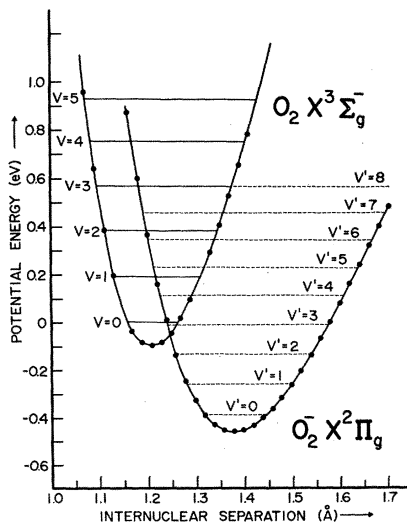


FIG. 2. Potential-energy curves for  $O_2$  and for  $O_2^-$ .

eV or  $32\,934\text{ cm}^{-1}$ .

This potential-energy diagram for  $O_2^-$  differs from that presented by Herzberg,<sup>23</sup> who used a curvature based upon the vibrational frequency of the  $O_2$  species and an equilibrium internuclear separation found by comparison of the corresponding differences between the equilibrium internuclear separations of the systems  $O_2-O_2^+$  and  $NO-NO^+$ . This potential-energy diagram also differs from that presented by Conway<sup>24</sup> who located the height of the lowest vibrational level of  $O_2^-$  0.06 eV above the ground state of  $O_2$  and who used the method of successive approximations to derive  $r_e$  and  $k_e$  from Badger's relation<sup>20</sup> and the Lippincott relation,<sup>25</sup> respectively.

## VII. DISCUSSION

The potential-energy curve of Fig. 2 can be used for an interpretation of three-body attachment in  $O_2$ . This process proceeds<sup>24</sup> via vibrationally excited levels of the negative ion. Figure 2 suggests that

attachment occurs initially by transitions from  $O_2$  ( $\nu=0$ ) to  $O_2^-$  ( $\nu'=4$ ) and higher-lying levels of  $O_2^-$ . Subsequent stabilization by a third body removes excess energy causing transitions to nonautoionizing levels of the ion, namely,  $\nu'=0, 1, 2,$  and  $3$ .

The potential-energy curve of Fig. 2 also offers the possibility of predicting photodetachment cross sections by calculating the relevant Franck-Condon factors.

The lifetime of the compound state determines the role played by this species in collision events. Using resonance theory and the integrated cross sections for vibrational excitation given by Hake and Phelps,<sup>26</sup> Herzberg<sup>23</sup> has estimated the lifetime of the compound state to be of the order  $10^{-10}$  sec. This estimate is within the range  $10^{-13}$ – $10^{-10}$  sec deduced by Chanin, Phelps, and Biondi,<sup>27</sup> from drift-tube studies of attachment of slow electrons in  $O_2$ .

Usually in order to more rigorously identify the configuration of the compound state, it is necessary to determine the angular dependence of the scattering. It is possible to predict by considering conservation of angular momentum and parity that if the configuration involved is  $O_2^- \ ^2\Pi_g$ , then the observed angular dependence will be  $d$  wave modified by the two-center nature of the potential, provided that the lifetime is shorter than the rotational period of the molecule. Previous angular distribution studies in  $H_2$  and  $N_2$  have verified<sup>28</sup> the correlation between the observed angular distributions and those distributions predicted along the lines described above. However, in each of these cases the important condition that the lifetime be short compared with the rotational period has been satisfied. The lifetime estimates for  $O_2^-$  indicate that rotational effects will play an important role in determining the angular distributions and may also affect the nature of the structure observed in the differential cross section.

## ACKNOWLEDGMENT

The authors gratefully acknowledge many valuable suggestions received from A. Herzberg, D. Spence, F. R. Gilmore, and A. V. Phelps.

†Work supported by the National Science Foundation.

<sup>1</sup>G. J. Schulz, Phys. Rev. **135**, A988 (1964); Phys. Rev. Letters **10**, 104 (1963).

<sup>2</sup>M. J. W. Boness and J. B. Hasted, Phys. Letters **21**, 526 (1966).

<sup>3</sup>J. B. Halsted and A. M. Awan, J. Phys. B **2**, 367 (1969).

<sup>4</sup>D. Spence and G. J. Schulz, Phys. Rev. A **2**, 1802 (1970).

<sup>5</sup>R. S. Mulliken, Phys. Rev. **115**, 1225 (1959).

<sup>6</sup>D. R. Bates and H. S. W. Massey, Trans. Roy. Soc. (London) **A239**, 269 (1943).

<sup>7</sup>G. Herzberg, *Spectra of Diatomic Molecules* (Van Nostrand, Princeton, N. J., 1967).

<sup>8</sup>M. J. W. Boness, J. B. Hasted, and I. W. Larkin

[Proc. Roy. Soc. (London) **A305**, 493 (1968)] have suggested the existence of an excited bound state of  $O_2^-$  in order to resolve the discrepancy between their work and the solid-state results of Rolfe [J. Rolfe, J. Chem. Phys. **40**, 1664 (1964)]. However, the newer solid-state work (Ref. 9) removes this discrepancy and there is therefore no reason to invoke such an excited state of  $O_2^-$ .

<sup>9</sup>W. Holzer, W. F. Murphy, H. J. Bernstein, J. Rolfe, J. Mol. Spectry. **26**, 543 (1968).

<sup>10</sup>R. K. Curran, J. Chem. Phys. **35**, 1849 (1961).

<sup>11</sup>J. A. D. Stockdale, R. N. Compton, G. S. Hurst, and P. W. Reinhardt, J. Chem. Phys. **50**, 2176 (1969).

<sup>12</sup>G. J. Schulz and D. Spence, Phys. Rev. Letters **22**, 47 (1969); D. Spence and G. J. Schulz, Phys. Rev. **188**,

280 (1969).

<sup>13</sup>F. C. Fehsenfeld, D. L. Albritton, J. A. Burt, and H. I. Schiff, *Can. J. Chem.* **47**, 1793 (1969).

<sup>14</sup>D. B. Dunkin, F. C. Fehsenfeld, and E. E. Ferguson, *J. Chem. Phys.* **53**, 987 (1970).

<sup>15</sup>D. Vogt, B. Hauffe, and H. Neuert, *Z. Physik* **232**, 439 (1970).

<sup>16</sup>Below 3 eV, J. F. Paulson (private communication) finds that the reaction  $H^+ + O_2 \rightarrow O_2^+ + H$  has an endothermic character, whereas one would deduce an exothermic character from the region above 3 eV. It is the latter region that is studied in Ref. 15.

<sup>17</sup>D. S. Burch, S. J. Smith, and L. M. Branscomb, *Phys. Rev.* **112**, 171 (1958).

<sup>18</sup>S. Geltman, *Phys. Rev.* **112**, 176 (1958).

<sup>19</sup>J. L. Pack and A. V. Phelps, *Phys. Rev. Letters* **6**, 111, (1961); J. L. Pack and A. V. Phelps, *J. Chem. Phys.* **44**, 1870 (1966).

<sup>20</sup>R. M. Badger, *J. Chem. Phys.* **2**, 128 (1934); **3**, 710 (1935). We are indebted to R. S. Mulliken for drawing our attention to these papers.

<sup>21</sup>P. M. Morse, *Phys. Rev.* **34**, 57 (1929).

<sup>22</sup>F. R. Gilmore, *J. Quant. Spectry. Radiative Transfer* **5**, 369 (1965).

<sup>23</sup>A. Herzenberg, *J. Chem. Phys.* **51**, 4942 (1969).

<sup>24</sup>D. C. Conway, *J. Chem. Phys.* **36**, 2549 (1962).

<sup>25</sup>E. R. Lippincott and R. Schroeder, *J. Chem. Phys.* **23**, 1131 (1955).

<sup>26</sup>R. D. Hake, Jr., and A. V. Phelps, *Phys. Rev.* **158**, 70 (1967).

<sup>27</sup>L. M. Chanin, A. V. Phelps, and M. A. Biondi, *Phys. Rev.* **128**, 219 (1962).

<sup>28</sup>D. Andrick and H. Ehrhardt, *Z. Physik* **192**, 99 (1966); H. Ehrhardt, L. Langhans, F. Linder, and H. S. Taylor, *Phys. Rev.* **173**, 222 (1968).

PHYSICAL REVIEW A

VOLUME 2, NUMBER 6

DECEMBER 1970

## Properties of the $\pi^-$ - $^4\text{He}$ Atom as Determined from Low-Energy $\pi^\pm$ - $^4\text{He}$ Scattering Phase Shifts\*

J. H. Boyd<sup>†</sup>

*Department of Physics, Illinois Institute of Technology, Chicago, Illinois 60616*

(Received 9 February 1970)

An effective-range analysis is used to predict properties of the  $\pi^-$ - $^4\text{He}$  atom. The method produces precise predictions; however, our predictions are broadened because of systematic differences between phase shifts from the various scattering experiments. The bounds obtained for the  $1s$  and  $2p$  level shifts (due to the strong interaction) are 90 to 160 eV (toward less binding) and  $(-2.4$  to  $-4.0) \times 10^{-3}$  eV, respectively. The bounds obtained for the nuclear capture rates from the  $1s$  and  $2p$  states are  $(0.12$  to  $1.8) \times 10^{17}$  sec<sup>-1</sup> and  $(0.46$  to  $4.0) \times 10^{12}$  sec<sup>-1</sup>, respectively. The results are consistent with mesonic x-ray measurements.

Effective-range relations which take into account the presence of the Coulomb interaction<sup>1</sup> are used to predict various properties of the hydrogenlike  $\pi^-$ - $^4\text{He}$  atom from  $\pi^\pm$ - $^4\text{He}$  elastic-scattering phase shifts.<sup>2-4</sup> These properties include (a)  $s$ - and  $p$ -state atomic level shifts due to the strong interaction, (b) nuclear capture rates from  $s$  and  $p$  states, and (c) bounds on the relative intensities of some of the mesonic x-ray lines. The data used in this analysis are the  $l=0$  and  $l=1$  phase shifts from the  $\pi^\pm$ - $^4\text{He}$  elastic-scattering (counter) experiments of Nordberg and Kinsey<sup>2</sup> at 85 MeV/ $c$  and of Crowe *et al.*<sup>3</sup> at 130, 142, 153, and 163 MeV/ $c$ , and from the (bubble chamber) experiment of Block *et al.*<sup>4</sup> at 129, 140, and 150 MeV/ $c$ . By refitting the differential-cross-section data, we have verified that the published values of the phase shifts,<sup>2-4</sup> which we have used in our analysis, are satisfactory. This method of analysis was first used by us to obtain predictions from a  $K^-$ - $^4\text{He}$  elastic-scattering experiment,<sup>5</sup> but it has not been previously applied to  $\pi^-$ - $^4\text{He}$  scattering. The  $\pi^-$ - $^4\text{He}$  case is especially

interesting because more  $\pi$ -mesonic x-ray data are available for comparison<sup>6-8</sup> than in the  $K^-$ - $^4\text{He}$  case.

The relation between the (complex)  $s$ -wave scattering length  $A_0$  and the  $s$ -wave strong-interaction phase shift  $\delta_0$  is<sup>1</sup>

$$\frac{1}{B} \left[ \frac{C_0^2(\eta) \cot \delta_0}{\eta} - 2h(\eta) \right] = \frac{-1}{A_0} + \frac{1}{2} r_0 k^2 + O(k^4), \quad (1)$$

where  $B = \text{Bohr radius} = 100.6 \text{ F}$ ,  $\eta = 1/(kB)$ ,

$$k = P_{\text{c.m.}}/\hbar,$$

$$h(\eta) = \eta^2 \sum_{m=1}^{\infty} \frac{1}{m(m^2 + \eta^2)} - \ln \eta - 0.577,$$

$$C_l(\eta) = |\Gamma(l+1+i\eta)| e^{(1/2)\pi\eta}.$$

The relation between the  $s$ -state atomic level shifts  $\Delta E_0$  and  $A_0$  is<sup>9</sup>

$$\frac{\Delta E_{ns}}{E_{ns}} = \frac{-4}{n} \frac{A_0}{B}, \quad (2)$$

where  $n$  is the principal quantum number. The cor-